On the Fast Electron Beam, Consequent Generation of Electrostatic Fields and Fast Ion Production in Front of LH Grills: Measurements and Theory

V. Petržílka, F. Žáček, B. Kolman, F. Kroupa, K. Jakubka, J. Stoeckel, R. Klíma, L. Krlín, and P. Pavlo
Institute of Plasma Physics, P.O. Box 17, 182 21 Praha 8, Czech Republic
J. Gunn, M. Goniche, V. Fuchs, P. Devynck
Association Euratom-CEA, CEA/Cadarache, 13108 Saint Paul-lez-Durance, France
D. Tskhakaya 1), S. Kuhn
Department of Theoretical Physics, University of Innsbruck, Austria
1) Permanent address: Institute of Physics, 380077 Tbilisi, Georgia
J. A. Tataronis
University of Wisconsin, 1500 Engineering DR, Madison, WI 53706, USA
J. Lorincik
Institute of Physical Chemistry, Dolejškova 3, 182 23 Praha 8, Czech Republic

e-mail contact of the main author: vap@ipp.cas.cz

Abstract: The paper presents measurements of radial variations of the floating potential at the Tore Supra (TS) tokamak ergodic divertor plate and in front of the CASTOR tokamak lower hybrid (LH) grill, due to the presence in these two locations of the fast particle beam generated in front of LH grills. The paper also presents a scanning electron microscope (SEM) and secondary ion mass spectrometric (SIMS) analysis of an eroded graphite tile from the TS LH grill guard limiter, performed in order to check the authors' theoretical conclusion that fast ions can be generated in a thin layer in front of LH grills and that they can contribute to damage of tokamak vessel components. The paper first presents theoretical conclusions that are relevant to the experimental data and then the experimental results.

1. Introduction

Thermal electrons can be accelerated in front of a lower hybrid (LH) waveguide array by the electric field of the slow LH wave [1, 2]. They may cause high thermal loads and erosion observed on parts of the grill and tokamak vessel. Without spontaneously generated fields in front of the LH grill mouth, this acceleration is limited to a narrow layer in front of the grill, where higher LH wave harmonics can propagate. However, as was theoretically demonstrated, the electron acceleration in front of the grill may be significantly enhanced by random fields, which are spontaneously generated near the antenna [3, 4]. Consequently, a strong stationary toroidal electric field E_z appears just in front of the grill structure as a result of the opposing actions of the plasma pressure gradient and the effective ponderomotive force emerging from the nonlinear electron acceleration. The potential U of this electrostatic field is defined by $E_z = - \delta U/\delta z$. Since U also varies radially and poloidally, radial and poloidal electrostatic fields also appear in front of the grill, $E_r = - \delta U/\delta r$ and $E_\theta = - \delta U/r\delta\theta$, respectively. A significant consequence of the charge-separation electrostatic field E_z is that it also accelerates ions [5]. This physical process is analogous to the so called Coulomb explosion in laser plasmas that are produced by dynamic electric fields in double layers [6]. To study this effect in more detail, we performed a series of simulations [5, 7, 8] with a Particle-in-Cell (PIC) code. Let us note that recent PIC simulations [9, 10] of the electron acceleration in the region near to the LH grill mouth, even if they are very successful in modeling of a variety of physical processes involved in the electron acceleration, cannot reveal the complex electrostatic field structure formation in front of the grill

and consequent generation of the fast ion beam. The simulation time of several nanoseconds used in [9] was too short, and ions were assumed to be infinitely heavy and have been replaced by a positive charge density constant in time in [10].

2. Fast Electron and Ion Beams

Because of the possible presence of a very thin evanescent layer at the grill mouth and because of a strong Landau damping at the plasma boundary, the high $k_{//}$ Fourier components of the wave field do not propagate into the plasma interior [10]. The radial scale length of the decrease of the spontaneously excited fields may be larger, about several cm. By using a test particle model, we computed variations of the resulting electron distribution functions as a function of the number of the higher Fourier components j in front of the grill mouth, and of the intensity of the spontaneously excited random fields.
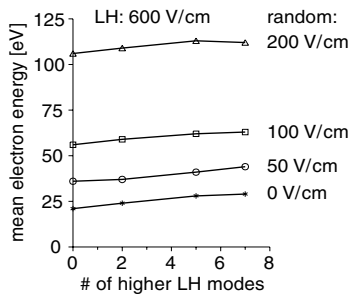

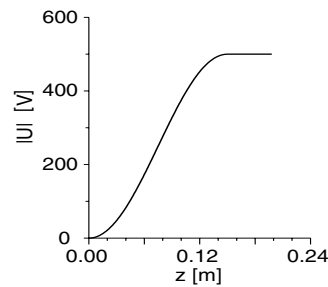Fig. 1: Dependence of the mean electron energy for the CASTOR tokamak on the LH modes # j.

Fig. 2: Dependence of U for Tore Supra; z=0 is in the poloidal symmetry plane of the grill.

For the CASTOR tokamak, the LH wave and grill parameters are specified as follows [11]: We take a four waveguide grill toroidally extending from z = -2.4 to z = 2.4 cm, and the width of individual waveguides is 1.2 cm. The computational results are very similar also for a three waveguide grill alternatively used in CASTOR. The wave frequency is 1.25 GHz, and the maximum electric field amplitude is 600 V/cm. In the computations, we follow the acceleration of an electron ensemble of 1000 electrons, with initial positions equidistantly distributed in front of the grill. Figure 1 shows the mean electron energy following from the resulting distribution functions, for a growing number of the Fourier components j, and for various random field amplitudes. For the TORE SUPRA tokamak, the LH wave and grill parameters are chosen as follows [2]: the frequency is 3.7 GHz, and the maximum electric field amplitude is assumed to be 5 kV/cm. Again, the injected electrons have randomly distributed initial velocities corresponding to the Maxwell velocity distribution with the temperature of 25 eV. We note that the JET grill parameters are similar, and consequently give similar results. As in CASTOR, we again computed the final accelerated electron energy, averaged over an ensemble of 1000 electrons. For the highest random field amplitude of 500 V/cm, the averaged accelerated electron energy is about 1000 eV. This value will be also used for the effective ponderomotive potential W expelling electrons from the space in front of the grill.

Using two-fluid equations, we consider a stationary equilibrium along the tokamak toroidal magnetostatic field, B_0. The direction of the z coordinate is aligned along B_0. The equilibrium arises due to the opposing actions of the plasma pressure gradient and the charge separation force arising from the nonlinear electron acceleration. First, we will consider the plasma

equilibrium in front of the grill mouth along the z coordinate for negligible values of the particle sources S. Figure 2 shows the variations of the electrostatic potential U. The maximum of the corresponding electrostatic field E_z is larger than 5 kV/m. Taking into account the maximum value of U, and the poloidal length of the waveguide row (of the order of 10 cm), we find that the maximum value of the corresponding poloidal electrostatic field E_θ is about 10 kV/m. This poloidal electrostatic field is directed from the poloidal symmetry line of a waveguide row to the poloidal sides of the row, and thus gives rise to a strong radial convection in front of the grill, which has radially opposite directions on the poloidally opposite sides of the waveguide row, and
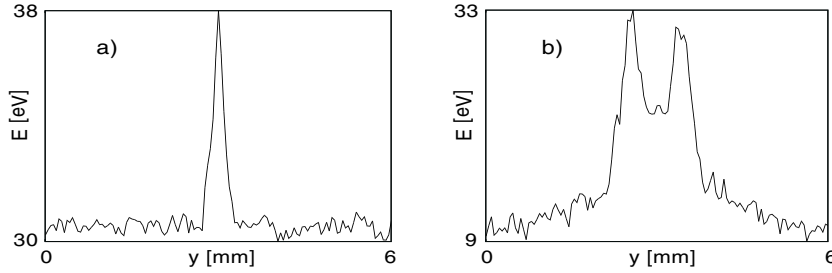

Fig. 3. Radial profiles of the average particle energy; a) electron and b) ion beams leaving the CASTOR grill. The radial scale in PIC modeling is 4x shortened, i.e., the modeled radial width is 4x6= 24 mm.

which is zero on the poloidal symmetry line of the waveguide row. For the tokamak toroidal magnetostatic field of about 3 T, the maximum value of this radial plasma velocity is about 3×10^3 m/sec. Similarly, the radial variation of the intensity of the electron acceleration gives rise to a strong radial electrostatic field in front of the grill, and to a corresponding poloidal plasma rotation. A similar plasma vortex, but of a significantly lower intensity, was studied in Ref. 12.

We also computed the flow of particles from the layer just in front of the LH grill for realistic values of sources S. In the two fluid MHD model, we found that the dimensionless flow velocity tends to reach values larger than the ion sound velocity and tends to produce discontinuities in the plasma density and in the outflow velocity in front of the grill mouth. To study the ion acceleration in 1-D and 2-D models in more detail, we performed a series of simulations [5, 7, 8] with the PIC code. As in the two-fluid model, the ponderomotive potential W acts on all electrons also in the PIC model, and the ions are then again accelerated by the charge-separation electric field. Figure 3 shows the radial profiles of the electron and ion beams in front of the CASTOR grill, obtained by the PIC computations.

3. Probe Measurements on CASTOR and TORE SUPRA

Using movable Langmuir probes, we measured a potential difference of up to about –150 Volts in the first 2 mm radially in front of the CASTOR LH grill mouth for the maximum LH power available on CASTOR. The probe floating potential, which exhibits a strong decrease during LHW power launch, thus confirms the presence of the fast electrons just in front of the grill mouth. The decrease has the form of a well localized radially in the very narrow layer in front of the grill. The depth of the well grows linearly with growing LH power.

On TORE SUPRA, LH power at a level of 2 MW was injected into an ergodic divertor discharge with toroidal field 3 T and plasma current 1.4 MA. When the divertor is activated, the midplane neutralizer plate D6 of module PJ6 is magnetically connected to the adjacent antenna C2 with a connection length of about 1.3 m, as shown in Fig. 4. Four domed Langmuir probes, 2 mm high,

are mounted on this neutralizer plate. Depending on the radial position of the antenna and on the magnitude of the divertor current, the probes can be connected either to the antenna sides, or to
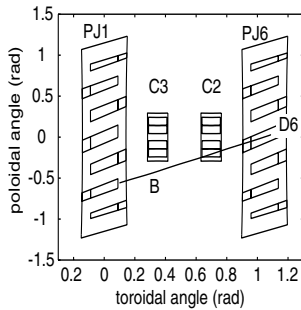

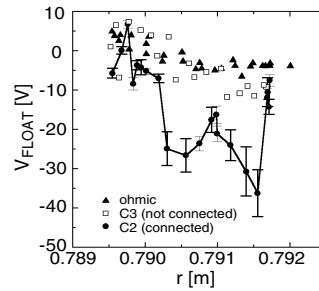Fig. 4. Schematic view of the TS LH grills and ergodic divertor configuration.

Fig. 5. Potential decrease measured in the beam at the ergodic divertor plate.

the region in front of the grills, and hence to any beam of charged fast particles that might be generated there. In order to obtain the radial profile of the beam, the connected zone was swept over Langmuir probe D6b by modulating the divertor current. The results are shown in Fig. 5. There is no change in the floating potential when C3 fires, since there is no magnetic connection to that grill. There is a change, however, when C2 fires. The measured floating potential exhibits a dip over a narrow range of divertor current. The floating potential drops about 30 V over a radial extent of about 1.5 mm. The relatively low value of 30 Volts can be due to slowing down of fast electrons leaving the space in front of the grill by the positive charge remaining in front of the active grill, cf. also Fig. 3. As the CASTOR measurements are performed just in front of the grill, the measured values of the potential well are higher, in spite of lower energy of the accelerated electrons in CASTOR. The radial extent of the potential well on CASTOR and Tore Supra is approximately the same, in agreement with PIC computations in Fig. 3.
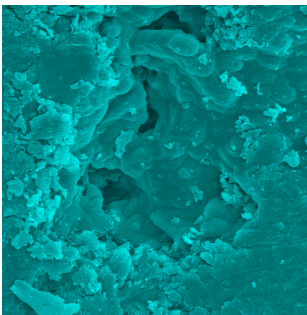

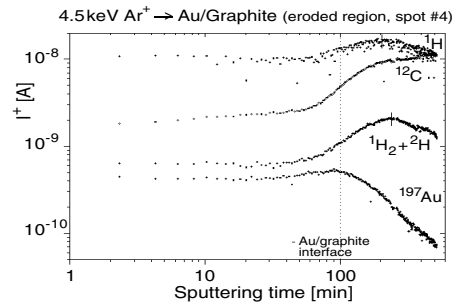Fig. 6. SEM photography of an eroded location on the graphite tile (1000x).

Fig. 7. Typical SIMS result from an eroded location of the graphite tile. The sample was covered by a gold layer prior to SIMS analysis.

4. Erosion of a Graphite Tile from the LH Grill Guard Limiter

In the following, we briefly describe a Scanning Electron Microscope (SEM) and Secondary Ion Mass Spectrometry (SIMS) analysis of eroded locations of the graphite tile exposed to the fast particle beam in the guard limiter of the TORE SUPRA LH grill. The tile was eroded by several mm in the most eroded spot. Figure 6 shows a typical view of the eroded location of the graphite

tile. The tile was covered by a thin gold layer for higher SEM contrast. Erosion of this type may result from overheating by the locally accelerated electron and/or ion beam, and/or from sputtering by accelerated ions (the electrons with energy up to about 5 keV have too low momentum for sputtering). Figure 7 then shows typical SIMS results from more eroded regions of the graphite tile. The results confirm the presence of the plasma (H and D) ions in the tile surface. However, the depth resolution of the SIMS apparatus was too low (due to a crater effect) to allow it to be concluded from the depth profiles that the observed plasma ion presence in the tile material results from accelerated ion impact, and is not due simply to the presence of plasma thermal ions. Further observations should therefore be performed with a SIMS device, which would allow a higher depth and spatial resolution.

5. Conclusions

The key theoretical result is that the observed erosion in places magnetically connected to the LH grill mouth can result at least partially from sputtering by locally accelerated ions. The charge separation electrostatic field in front of the grill, created by an accelerated electron beam, can also be a cause of a significant plasma rotation (in addition to the ion acceleration along the magnetostatic field lines). The probe measurements on CASTOR and TORE SUPRA show a very narrow radial width of the fast electron beam. The magnitude of the measured potential well is up to about -150 Volts. These observations are in a qualitative agreement with our theoretical modeling results. The SEM and SIMS observations confirm that the erosion of the TORE SUPRA graphite tile damaged by the beam may be due to overheating by the particle beam and/or to locally accelerated ion beam sputtering. Further experiments are needed to investigate the role of the ion sputtering, as it is predicted by theory.

References

[1] V. Fuchs, M. Goniche, Y. Demers, P. Jacquet, and J. Mailloux: Phys. Plasmas 3 (1996) 4023.
[2] M. Goniche, D. Guilhem, P. Bibet, P. Froissard, et al.: Nuclear Fusion 38 (1998) 919.
[3] J. A. Tataronis and V. Petržílka: 1998 Sherwood Conference, Atlanta, oral paper 2D02.
[4] V. Petržílka et al.: invited paper, Varenna Fusion Theory Workshop 1998, p. 95 .
[5] V. Petržílka, D. Tskhakaya, J. A. Tataronis, S. Kuhn, et al.: 2nd Workshop on Role of Electric Fields, Maastricht, June 19 - 20, 1999, Czech. J. Phys. 49, S3 (1999) 127 - 140.
[6] H. Hora: Laser and Particle Beams 3, Part 1 (1985) 59 – 78.
[7] F. Žáček, V. Petržílka, K. Jakubka, J. Stoeckel, D. Tskhakaya and S. Kuhn: Book of Abstracts, 27th EPS Conf. Contr. Fusion and Plasma Phys., Budapest, 12-16 June 2000, p. 349.
[8] D. Tskhakaya, S. Kuhn, and V. Petržílka: ibid, p. 107.
[9] K. M. Rantamaeki et al.: Phys. Plasmas 5 (1998) 2553.
[10] K. M. Rantamaeki et al.: Plasma Phys. Control. Fusion 41 (1999) 1125 - 1133.
[11] F. Žáček et al.: Plasma Phys. Control. Fusion 41 (1999) 1221 - 1230.
[12] R. W. Motley and J. Glanz: Phys. Fluids 25 (1982) 2107.